Institute of Transportation Studies
University of California at Berkeley

Improved Data Measurement Using Existing Loop Detectors

Benjamin Coifman

WORKING PAPER
UCB-ITS-WP-99-4

July 1999
ISSN 0192 4141

Improved Data Measurement Using Existing Loop Detectors

Benjamin Coifman

University of California
Institute of Transportation Studies
109 McLaughlin Hall
Berkeley, CA 94720

zephyr@cs.berkeley.edu

(510) 848-5121

Abstract

This paper develops an improved algorithm for estimating velocity from isolated loop detector data. Unlike preceding works, the algorithm is simple enough that it can be implemented using existing controller hardware. The discussion shows how the benefits of this work extend to automated tests of detector data quality at dual loop speed traps. Finally, this paper refutes an earlier study that found conventional isolated loop velocity estimates are biased.

Keywords: traffic surveillance, single loop detectors, velocity estimation, data screening

Introduction

Loop detectors are the preeminent vehicle detector for freeway traffic surveillance. They are frequently deployed as isolated detectors, i.e., one loop per lane per detector station. Although isolated loops have been used for decades, debate continues on how to interpret the measurements and how to calibrate the detectors. This paper will provide a new perspective by clarifying the source of several errors and suggesting ways to eliminate these errors. The body of this work emphasizes velocity estimation, but it has implications for tests of detector data quality as well.

The first section of this paper reviews the state of the practice for parameter measurement and estimation from isolated loop detectors. The next section illustrates how conventional practice may be susceptible to changes in the vehicle population throughout the day as well as errors due to sample size. The paper continues by developing an algorithm to overcome these problems. Finally, the discussion shows how the work has implications for tests of detector data quality and elucidates the findings of an earlier study that concluded that isolated loop velocity estimates are biased.

Parameter Measurement and Estimation

Conventional isolated loop detectors are capable of measuring flow, the number of vehicles that pass the detector during a fixed sample period, and occupancy, the percentage of the given sample period that the detector is "occupied" by vehicles. For each lane, these two parameters are defined as:

$$q_k = \frac{n_k}{T} \tag{1A}$$

$$\theta_k = \frac{\sum_{j \in J_k} t_j}{T} \tag{1B}$$

where the subscript "k" indicates the given sample, subscript "j" indicates vehicle specific parameters and

q_k = flow during sample k

θ_k = occupancy during sample k

n_k = number of vehicles that pass the detector during sample k

T = sampling period

J_k = set of all vehicles that pass the detector during sample k

t_j = vehicle j's *on time*.

Two interdependent vehicle parameters are of interest for estimating mean sample velocity: vehicle velocity and vehicle length. Consider a single vehicle passing over a loop detector, as shown in Figure 1, the relationship between the vehicle's length and velocity is simply:

$$L_j = L_j^v + L_j^s = v_j \cdot t_j \tag{2}$$

where

L_j = vehicle j's effective length as "seen" by the detector

L_j^v = vehicle j's true length

L_j^s = length of detector's sensitivity region for vehicle j

v_j = vehicle j's velocity

The length of the detector's sensitivity region typically depends on many variables such as the vehicle's position in the lane, height of the vehicle's underframe, and the amount of ferrous metal in the vehicle. It is difficult to separate this length from the vehicle's true length using loop detector data, so for the rest of this paper "length" will refer to the sum of these two lengths, often referred to as the effective vehicle length.

From equations 1 and 2,

$$\theta_k = \frac{1}{T}\sum_{j\in J_k}\frac{L_j}{v_j} = q_k \cdot \frac{1}{n_k}\sum_{j\in J_k}\frac{L_j}{v_j} \tag{3A}$$

assuming that individual vehicle lengths and velocities are uncorrelated,

$$\theta_k \approx \frac{q_k \cdot \overline{L}_k}{\overline{v}_k} \tag{3B}$$

where

$\overline{L}_k$ = arithmetic mean vehicle length for sample k

$\overline{v}_k$ = harmonic mean vehicle velocity for sample k, often referred to as the *space mean speed*.

In other words,

$$\overline{v}_k \approx \frac{q_k \cdot \overline{L}_k}{\theta_k} \tag{4}$$

Equation 4 shows the relationship between mean velocity and mean length, but these two parameters can not be measured independently at an isolated loop. Typically, an operating agency will use one of two approaches to address this problem, in the first case, $\overline{L}_k$ is simply set to a constant value, $\hat{L}$, and Equation 5 is used to estimate $\overline{v}_k$:

$$\hat{v}_k = \frac{q_k \cdot \hat{L}}{\theta_k} \tag{5}$$

But there are many site specific variables that can influence the mean vehicle length, such as the percentage of long vehicles at the station, percentage of long vehicles in the lane and the detector's sensitivity. So, other municipalities assume a fixed free flow velocity and reversing the

assignment in Equation 5, estimate $\hat{L}$ each day during periods when traffic over the detector is almost certain to be free flowing. Then, $\hat{L}$ is held fixed during the remainder of the day and the velocity estimation progresses using Equation 5 directly.

Analysis

Some of the site specific variables are corrected with a daily estimate of $\hat{L}$, but other factors are not addressed, such as the possibility that the percentage of long vehicles may change during the day or the simple fact that a sample with few vehicles (i.e., low flow) may not have a representative sample of vehicle lengths. For this study, we examine how $\overline{L}_k$ change throughout the day for each lane at a detector station on Interstate-80 in Berkeley, California. The raw data used for this study consists of 24 hours of detector actuations sampled at 60 Hz. Rather than using isolated loop detectors, the data come from dual loop *speed traps*; where a speed trap consists of two closely spaced loop detectors in the same lane. In this configuration, it is possible to measure true vehicle velocities by dividing the loop separation by the difference in arrival times at each loop. Finally, $\overline{L}_k$ is calculated using Equation 4 and assuming absolute equality.

Figures 2A and 3A[1] illustrate the time series evolution of $\overline{L}_k$ for $T = 15\,\text{min}$. The values of $\overline{L}_k$ range from 19 feet to 51 feet and almost all lanes exhibit a strong temporal dependency. Following Caltrans convention, lanes are numbered starting with one at the inside and increasing outward. At this location, lane 1 northbound and lanes 1-2 southbound exhibit lower $\overline{L}_k$ values because trucks are restricted from these lanes. The legend indicates the total number of vehicles in each lane during the day. Parts B-C of these figures show the corresponding n_k and $\overline{v}_k$, respectively, for the given directions. One can clearly see the velocities decrease with increasing lane number

When an operating agency estimates $\hat{L}$, they typically sample the value during early morning hours. As one would expect, these hours are free flowing for this example, however, they also correspond to the highest true values of $\overline{L}_k$. Furthermore, the flows are lowest during this period, with no vehicles observed in lane 1 southbound for over three hours. Thus, if $\hat{L}$ were estimated strictly during the early morning, estimates of velocity from Equation 5 would be too high throughout the remainder of the day. Since the phenomena depend on site specific factors, one

[1] Note that the vertical scale is different in the two figures to show as much detail as possible.

should not attempt to calculate correction factors from these data, rather, the figures indicate the need for an improved method of estimating $\hat{L}$.

Removing the temporal component, Figure 4 shows the cumulative distribution of $\bar{L}_k$ for the northbound lanes using four different sampling periods: $T = 30\,\text{sec}$, $T = 1\,\text{min}$, $T = 5\,\text{min}$, and $T = 15\,\text{min}$. Although the distributions are fairly tight for lane 1, the other lanes exhibit a large variance. So no single value of $\hat{L}$ will be representative of all samples. More importantly, a value of $\hat{L}$ estimated using one value of T may not be valid for another value of T.

The primary source of this variance comes from the fact that the vehicles observed during a given sample may not be representative of the entire vehicle population. Figure 5 shows the observed distribution of individual vehicle lengths, as calculated from Equation 2, for the northbound traffic. Approximately 85 percent of the vehicle lengths are between 15 and 22 feet, but some vehicles are as long as 80 feet or roughly four times the median length. Particularly during low flow, when n_k is small, a long vehicle can skew θ_k simply because it takes more time for the long vehicle to pass the detector.

In accordance with the Central Limit Theorem, the sample distribution should become more representative of the entire population as n_k increases, which in turn, increases with q_k and with T. Figure 6 illustrates this phenomena using the northbound data from all lanes for three different values of T. The top half of the figure shows $\bar{L}_k$ during free flow conditions, $\bar{v}_k$ > 50 mph, while the lower half shows $\bar{L}_k$ during congestion, $\bar{v}_k$ < 50 mph. The mean value of $\bar{L}_k$ is indicated for the data in each plot. In parts A and D, where $T = 30\,\text{sec}$, the maximum number of vehicles per sample is so small that the observations fall into distinct columns, i.e., the first column contains observations with only one vehicle, the second column contains observations with only two vehicles, and so on. Notice that for each value of T, the range of $\bar{L}_k$ decreases as q_k increases, also note that the lowest flows are only observed during free flow conditions in this data set.

Estimating Sample Velocity

As previously noted, an isolated loop detector can not measure $\bar{v}_k$ directly and estimates of $\hat{L}$ may be biased by the time of day. This section develops a methodology to overcome these problems. Like conventional practice, $\hat{L}$ is estimated during periods when the traffic should be free flowing.

But rather than using a static period of the day chosen a priori for this estimation, the approach uses θ_k to identify free flowing periods. In particular, a sample is considered free flowing if

$$\theta_k < \theta_{threshold} \tag{6}$$

where $\theta_{threshold} = 10\%$ for this study. To account for transient samples with high θ_k due to free flowing trucks, for $T = 30\,\text{sec}$, a sample is also considered free flowing if at least half of the 10 preceding samples satisfy Equation 6. Next,

$$\hat{L} = v_{ff} \cdot mean\left(\frac{q_k}{\theta_k}\right), \text{ over all } k \in K \tag{7}$$

where

v_{ff} = assumed fixed free flow velocity, set to 60 mph for this study

K = set of all free flow samples with $q_k > 0$ and $\theta_k > 0$ in the given lane during the 24 hour study.

The resulting $\hat{L}$ for the northbound traffic are shown in Table 1. Using these values and Equation 5 to calculate $\hat{v}_k$, Figure 7 shows $\hat{v}_k$ versus $\bar{v}_k$ for the northbound lanes over entire 24 hour study. The solid line in each plot indicates where the estimated values equal the measured values. Note that $\hat{v}_k$ ranges between 20 mph and 120 mph for samples with $\bar{v}_k > 50$ mph. In other words, the estimate is very noisy when the traffic is free flowing. Finally, consider the congested observations, $\bar{v}_k < 50$ mph. In each lane the observations are roughly collinear. The guess of v_{ff} serves as a scaling factor, increasing or decreasing the slope of the congested data. In lane 1, the guess of v_{ff} was too low and the estimated velocities are lower than the measured velocities, while in lanes 3 and 4, the opposite is true. This error is included in the plots because it can not be eliminated from an isolated loop data without additional detectors.

The analysis is repeated with $T = 5\,\text{min}$ to reduce the estimate noise. Now, however, a sample is only considered free flowing if it satisfies Equation 6 or the preceding sample satisfied Equation 6. Once more the resulting $\hat{L}$ are shown in Table 1, while Figure 8 shows $\hat{v}_k$ versus $\bar{v}_k$ for the northbound lanes with $T = 5\,\text{min}$. Even with the longer sampling period, the estimates are still noisy when the traffic is free flowing.

To illustrate the effects of different values of v_{ff} or $\hat{L}$, Figures 9 and 10 show contour plots of the cumulative distribution of the percent error as $\hat{L}$ ranges between 16 and 32 feet for two different lanes when (A) $T = 30\,\text{sec}$ and (B) $T = 5\,\text{min}$. For example, when $\hat{L}$ = 19 feet in Figure 9A, approximately 70 percent of the estimated velocities are within 5 percent of the measured values. Comparing part B to part A in either lane, at the longer sampling period, the error is reduced due to increased n_k. Notice that the optimal value of $\hat{L}$ appears to depend on T in Figure 10, reaffirming the fact that $\hat{L}$ estimated at one value of T may not be valid for another value of T.

Improving the Velocity Estimates

In Figures 7-8, when $\bar{v}_k$ > 50, most of the estimation errors are due to the large range of $\bar{L}_k$ at low q_k. From an operational stand point, it is sufficient to know that traffic is free flowing rather than knowing the true velocity during free flow conditions. This supposition is implicit with on-line estimation of $\hat{L}$. It would be desirable to identify the free flow, low flow, $q_k < q_{threshold}$, samples and simply assign $\hat{v}_k = v_{ff}$ for these periods. But one can not simply use q_k to identify these samples since a given value of q_k can correspond to two traffic states, one free flowing and the other congested, as shown in Figure 11. Fortunately, Equation 3 shows that θ_k monotonically increases as $\bar{v}_k$ decreases. So rather than using a flow based constraint, one can identify the free flow data via $\theta_k < \theta_{threshold}$. Rewriting Equation 5 to include this constraint yields Equation 8:

$$\hat{v}_k = \begin{cases} \dfrac{q_k \cdot \hat{L}}{\theta_k}, & \theta_k \geq \theta_{threshold} \\ v_{ff}, & \theta_k < \theta_{threshold} \end{cases} \tag{8}$$

To illustrate the benefits of this thresholding, return to the data in Figure 8. Recalculating $\hat{v}_k$ using Equation 8 with $\theta_{threshold} = 10\%$, the new relationships are shown in Figure 12. Notice that almost all of the noise has been eliminated from the estimates corresponding to samples with $\bar{v}_k$ > 50 mph. Figure 13 compares the time series $\hat{v}_k$ "before cleaning" from Equation 5, "after cleaning" from Equation 8, and $\bar{v}_k$. In this figure, one can see that cleaning removed many erroneous velocity estimates, particularly during the early morning. Repeating this exercise for the southbound data yields Figure 14. One can also apply this cleaning method to the 30 second data with similar results, Figure 15.

Implementation

The analysis for $T = 30\,\text{sec}$ used a moving average to identify free flow periods with high θ_k, but a moving average is memory intensive. In contrast, exponential filtering can accomplish the same goal with almost no data storage. The following code can be used to implement the theory presented in the preceding section:

if $\theta_k > 0$ and $q_k > 0$

  if $\theta_k < 10\%$ or $u > 0.1$

    $\hat{L} = v_{ff} \cdot mean\left(\frac{q_k}{\theta_k}\right) \cdot r + g \cdot (1 - r)$

    $\hat{v}_k = v_{ff}$

    $u = 1 \cdot p + u \cdot (1 - p)$

  else

    $\hat{v}_k = \frac{q_k \cdot \hat{L}}{\theta_k}$

    $u = 0 \cdot p + u \cdot (1 - p)$

  end

end

where

u = an indicator variable

r = filtering factor with a time constant on the order of 24 hours, e.g., $r = 1/2880$ for $T = 30\,\text{sec}$ and $r = 1/288$ for $T = 5\,\text{min}$.

p = filtering factor with a time constant on the order of 5 minutes, e.g., $p = 0.2$ for $T = 30\,\text{sec}$ and $p = 1$ for $T = 5\,\text{min}$.

Note that rather than using a static assignment of $\hat{L}$, as in Equation 7, the algorithm uses an exponential filter to dynamically update $\hat{L}$.

Discussion

Although the implementation is fairly simple, this work has wide ranging implications for practitioners and researchers.

Implications Beyond Isolated Loop Velocity Estimates

The impact of this work to isolated loop detectors is straight forward, but this work has implications for dual loop speed traps as well. Earlier studies have developed automated tests of detector data quality, e.g., [1-3]. Their goal is to eliminate erroneous measurements due to transient problems or component failures. Similar systems often go undocumented in the literature because they are either designed in-house by an operating agency or a consulting firm (see [4] for examples). Most of these data quality tests can be expressed using the following constraint to bound *good* speed trap data:

$$\bar{v}_k \in \left[\frac{q_k \cdot L_{\min}\left(q_k, \bar{v}_k, \theta_k\right)}{\theta_k}, \frac{q_k \cdot L_{\max}\left(q_k, \bar{v}_k, \theta_k\right)}{\theta_k} \right] \tag{9A}$$

where $L_{\min}$ and $L_{\max}$ are lower and upper bounds, respectively, that may depend on q_k, $\bar{v}_k$ or θ_k. Naturally, this constraint reduces to the following for isolated loop data:

$$\hat{v}_k \in \left[\frac{q_k \cdot L_{\min}\left(q_k, \theta_k\right)}{\theta_k}, \frac{q_k \cdot L_{\max}\left(q_k, \theta_k\right)}{\theta_k} \right] \tag{9B}$$

Some of these tests fail to accommodate the fact that the variance in $\bar{L}_k$ increases as q_k decreases. The author recently identified such a system currently in use by a large operating agency. In particular, the agency applies Equation 9A to speed trap data. The test discards almost all early morning observations from the agency's 400 detector stations simply because the constraint is too restrictive during low occupancy conditions.

Previous Research in the Context of the new Analysis

Many researchers have sought better estimates of velocity from isolated loops, e.g., [5-7]. Considering the performance of Equation 5 shown in Figure 15A, this search is justified. Unfortunately, most of the preceding efforts focused on complicated models, losing sight of the end goal: to produce an algorithm that can be deployed on a simple processor, such as a Model 170 controller[2].

[2] When Model 2070 controllers are eventually deployed for freeway surveillance, they may be powerful enough to implement the earlier works.

Of greater concern, there has been some confusion in the discipline since Hall and Persaud [8] concluded that, for a fixed value of $\hat{L}$, Equation 5 does not hold over an extended range of occupancies. In particular, they examined the "g-factor", where,

$$g = \frac{1}{\bar{L}_k} \tag{10}$$

Roughly summarizing their plots of g versus occupancy: g decreases by a factor of two from one percent to five percent occupancy, remains constant over the range of five percent to 40 percent occupancy, and then drops by an order of magnitude from 40 percent to 80 percent occupancy. To reduce errors due to vehicle lengths, they selected lanes with truck restrictions. In an attempt to reproduce these results, Figure 16A shows the g-factor versus occupancy for lane 1 northbound. The g-factor does not exhibit the predicted occupancy dependence. There is one difference, however, the earlier study used occupancy expressed in integer percent. After rounding percent occupancy down to integer values and recalculating g, Figure 16B shows the new g-factor versus integer percent occupancy. This plot exhibits the non-linearity at low occupancies predicted by Hall and Persaud, but it does not show the drop in g at high occupancy. Finally, using *time mean speed*[3] rather than *space mean speed* and the rounded occupancy to calculate g, Figure 16C follows the predictions from the earlier study. Figure 17 compares the various methods of calculating the g-factor on a single plot. The figure shows mean g-factor over one percent ranges up to 35 percent occupancy and then over five percent ranges through 50 percent occupancy. Note that by using *time mean speed* without rounding occupancy, the g-factor follows the predictions for high occupancy but it does not follow the predictions for low occupancy.

Although their diagnosis seems to be incorrect, Hall and Persaud correctly identified a significant problem with conventional velocity estimation. An operating agency should expect to encounter similar round off errors at low occupancy if they use integer percent occupancy to estimate $\hat{L}$ and this error will propagate to all subsequent velocity estimates. In the course of their analysis, Hall and Persaud assumed the operating agency was measuring *space mean speed* when in fact it appears that the agency was measuring *time mean speed*. This measurement error would explain their results at high occupancy. To prevent such oversights in the future, researchers should learn the subtle details of the data measurement and aggregation procedures underlying their detector data. One must remember that loop detectors, as well as most other vehicle detectors, are not precision instruments. To keep the detectors affordable, they are typically designed to meet

[3] The arithmetic mean of each samples' vehicle velocities.

existing operational needs with minimal excess performance. Finally, recall that the results in Figure 17 represent a lane with a truck restriction. As shown earlier in this paper, when trucks are present, the large range of possible vehicle lengths will reduce the accuracy of velocity estimates from isolated loops.

Conclusions

This paper developed an improved method for estimating $\hat{L}$, when compared to conventional practice, it is less sensitive to time of day trends in $\overline{L}_k$. In the process of deriving the method, it was shown that variance in $\overline{L}_k$ increases as q_k decreases. It was also shown that a value of $\hat{L}$ estimated using one value of T may not be valid for another value of T. Next, the paper developed a robust velocity estimate that reduces the errors at low q_k. Unlike many preceding works, the approach is simple enough that it can be implemented on existing traffic controllers that have limited processing power, such as a Model 170 controller.

The significance of this work to isolated loop detectors is straight forward. The discussion shows how the work is also applicable to automated tests of detector data quality, both from dual and single loop detectors. Then, the paper closes by refuting an earlier study, showing that Equation 5 does indeed hold over an extended range of occupancies provided care is taken to measure the right parameters and prevent round off errors.

References

[1] Jacobson, L, Nihan, N., and Bender, J., "Detecting Erroneous Loop Detector Data in a Freeway Traffic Management System," *Transportation Research Record 1287*, TRB, Washington, DC, 1990, pp 151-166.

[2] Cleghorn, D., Hall, F., and Garbuio, D., "Improved Data Screening Techniques for Freeway Traffic Management Systems," *Transportation Research Record 1320*, TRB, Washington, DC, 1991, pp 17-31.

[3] Nihan, N., "Aid to Determining Freeway Metering Rates and Detecting Loop Errors", *Journal of Transportation Engineering*, Vol 123, No 6, ASCE, November/December 1997, pp 454-458.

[4] Chen, L., and May, A., "Traffic Detector Errors and Diagnostics" *Transportation Research Record 1132*, TRB, Washington, DC, 1987, pp 82-93.

[5] Mikhalkin, B., Payne, H., Isaksen, L., "Estimation of Speed from Presence Detectors" Highway Research Record 388, HRB, Washington, DC, 1972, pp 73-83.

[6] Pushkar, A., Hall, F., Acha-Daza, J., "Estimation of Speeds from Single-Loop Freeway Flow and Occupancy Data Using Cusp Catastrophe Theory Model" Transportation Research Record 1457, TRB, Washington, DC, 1994, pp 149-157.

[7] Dailey, D., "A Statistical Algorithm for Estimating Speed from Single Loop Volume and Occupancy Measurements" Transportation Research-B, Vol 33B, No 5, June 1999, pp 313-322.

[8] Hall, F., Persaud, B., "Evaluation of Speed Estimates Made with Single-Detector Data from Freeway Traffic Management Systems" Transportation Research Record 1232, TRB, Washington, DC, 1989, pp 9-16.

Figure 1, Vehicle j passing over a loop detector. The height of the vehicle's trajectory reflects the non-zero vehicle length.

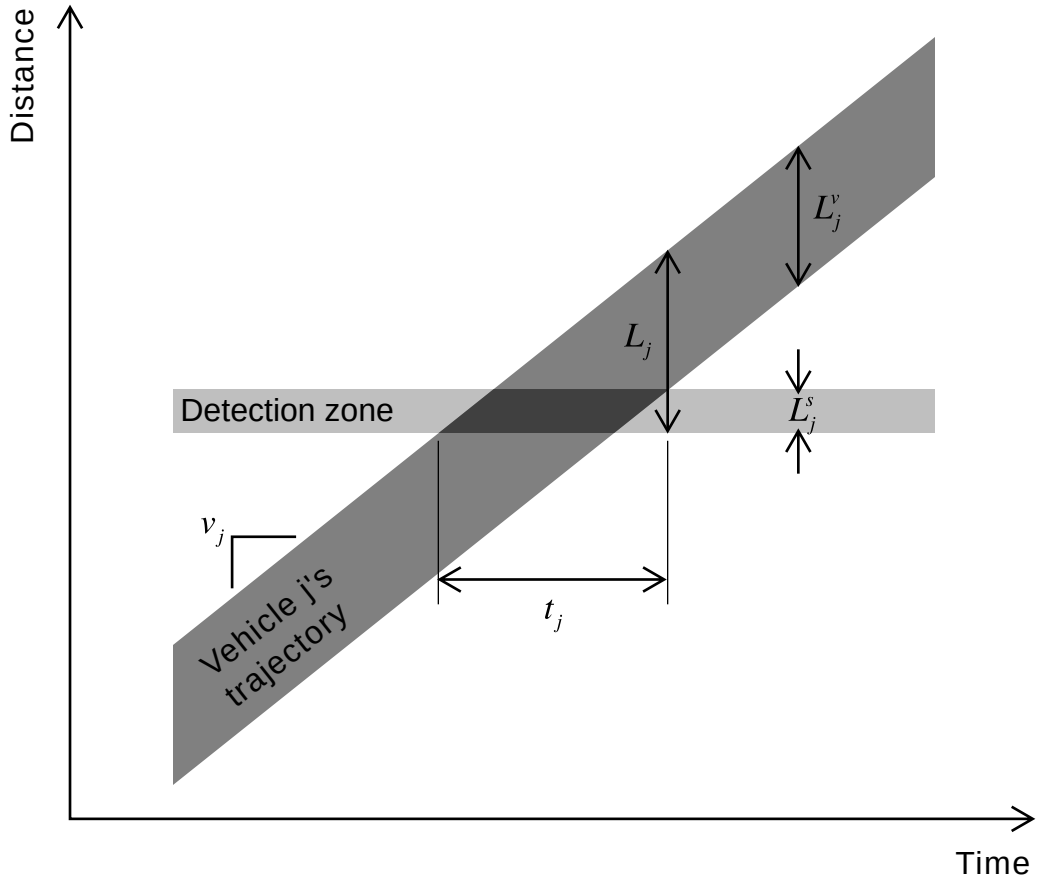

Figure 2, (A) True $\bar{L}_k$ by lane as a function of time for the northbound lanes, T = 15 minutes, and the corresponding (B) number of vehicles per sample (C) measured velocities.

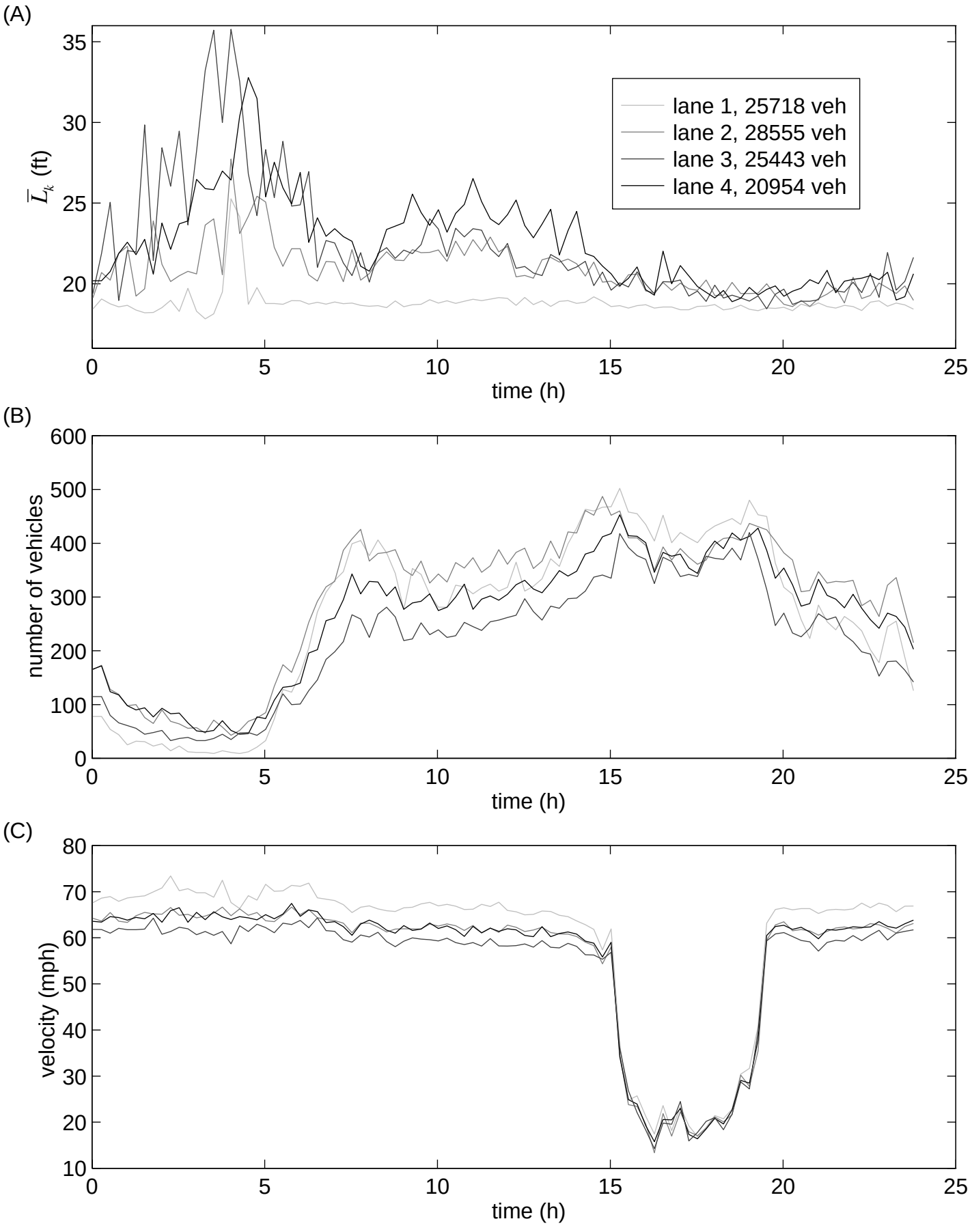

Figure 3, (A) True $\bar{L}_k$ by lane as a function of time for the southbound lanes, T = 15 minutes, and the corresponding (B) number of vehicles per sample (C) measured velocities.

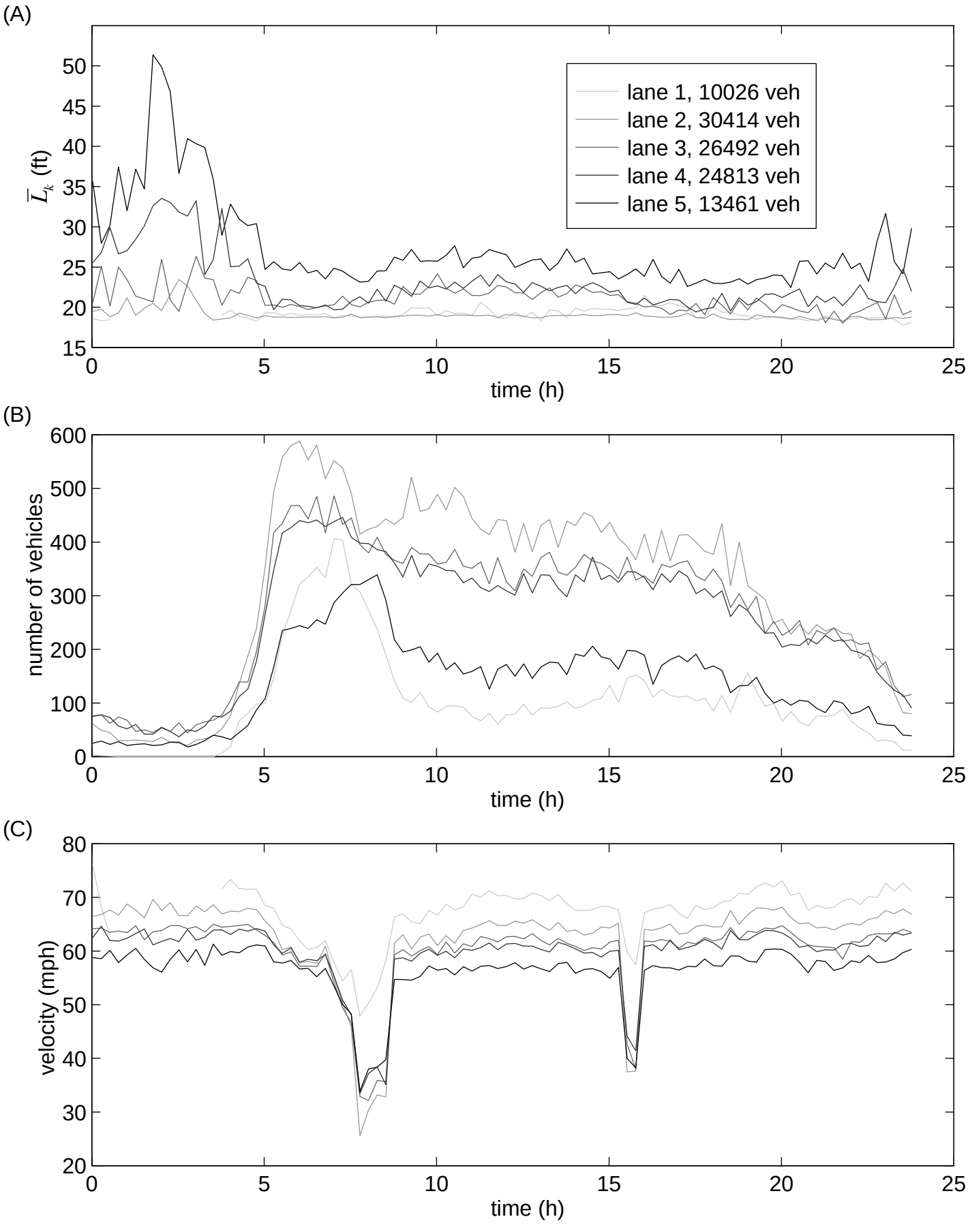

Figure 4, CDF of the true $\overline{L}_k$ over 24 hours for the northbound traffic, (A) lane 1 (B) lane 2 (C) lane 3 (D) lane 4.

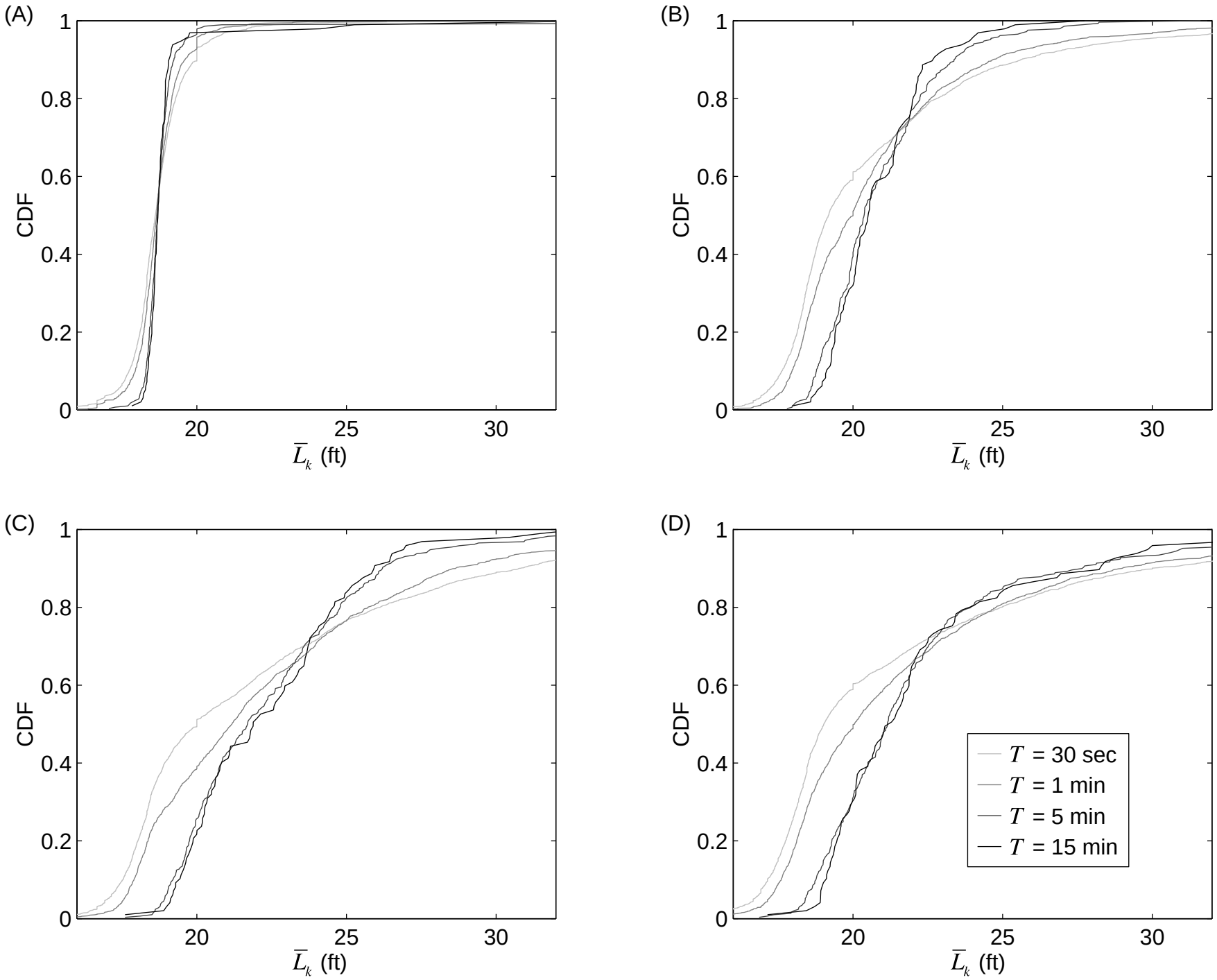

Figure 5, (A) Cumulative distribution of individual vehicle lengths, L_j, for the northbound lanes. (B) detail of part A.

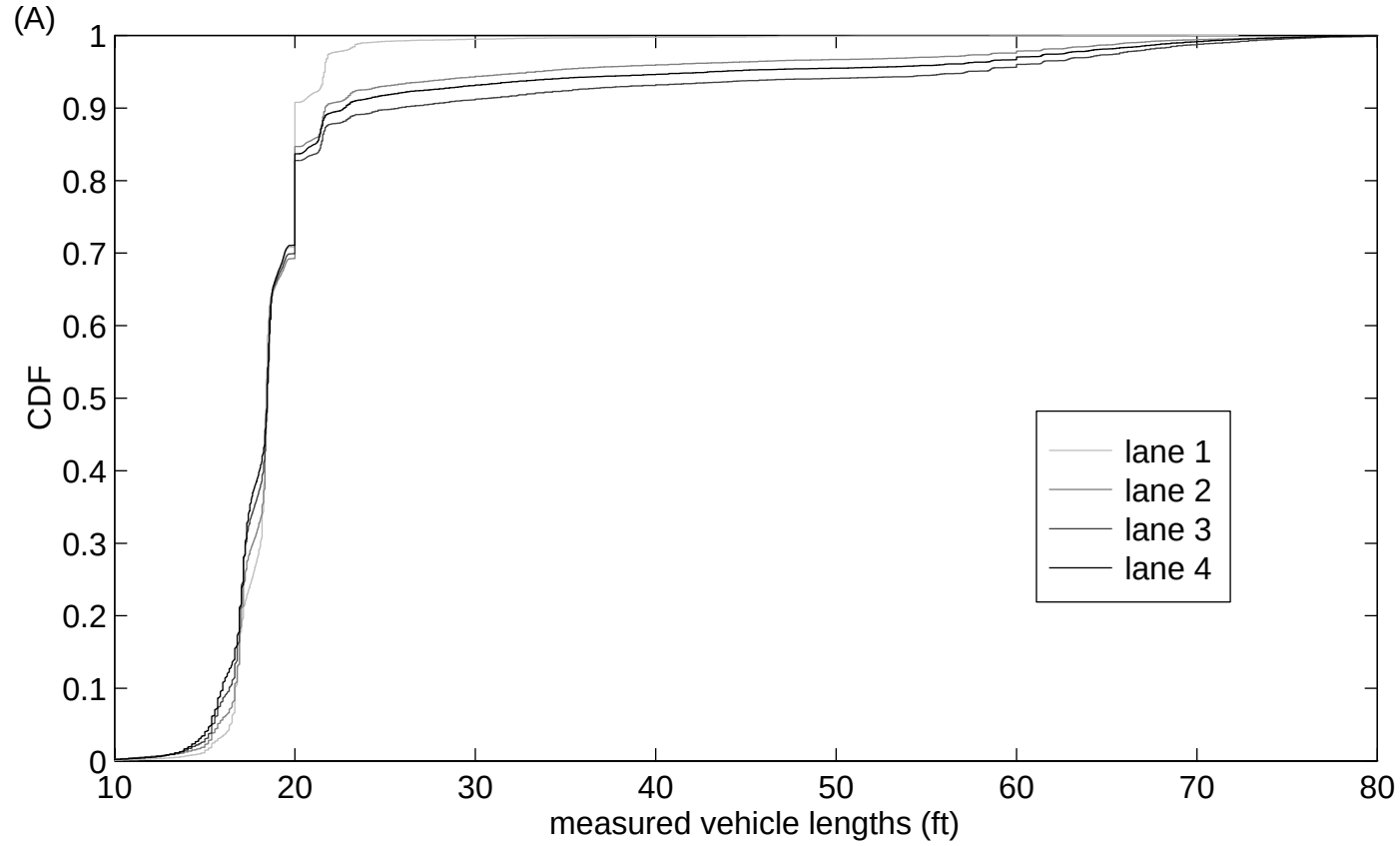

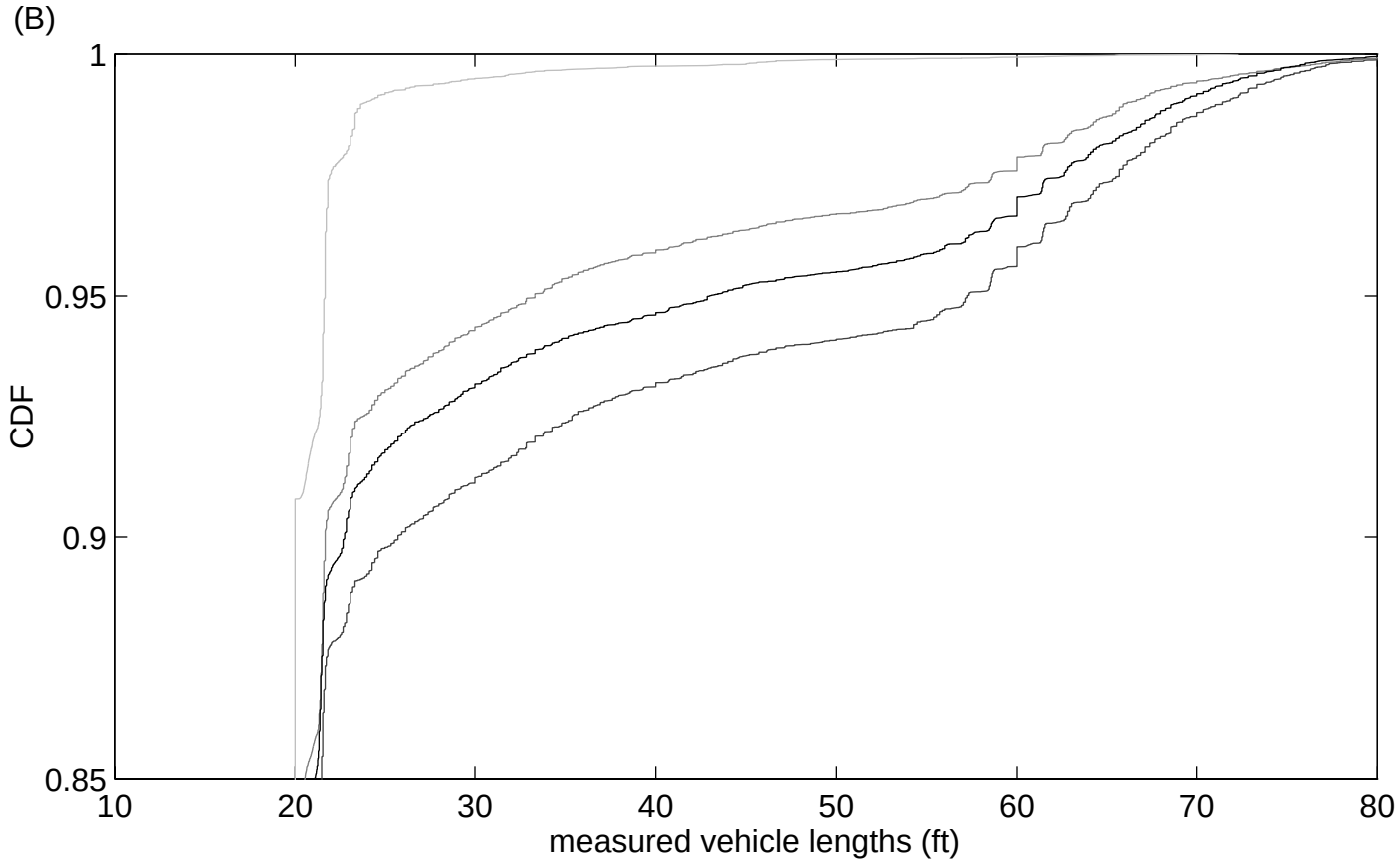

Figure 6, $\bar{L}_k$ versus flow, q_k, for the northbound traffic: (A)-(C) during free flow, $\bar{v}_k$ > 50 mph and (D)-(F) congestion, $\bar{v}_k$ < 50 mph; sampled at (A) & (D) T = 30 sec, (B) & (E) T = 5 min, (C) & (F) T = 15 min.

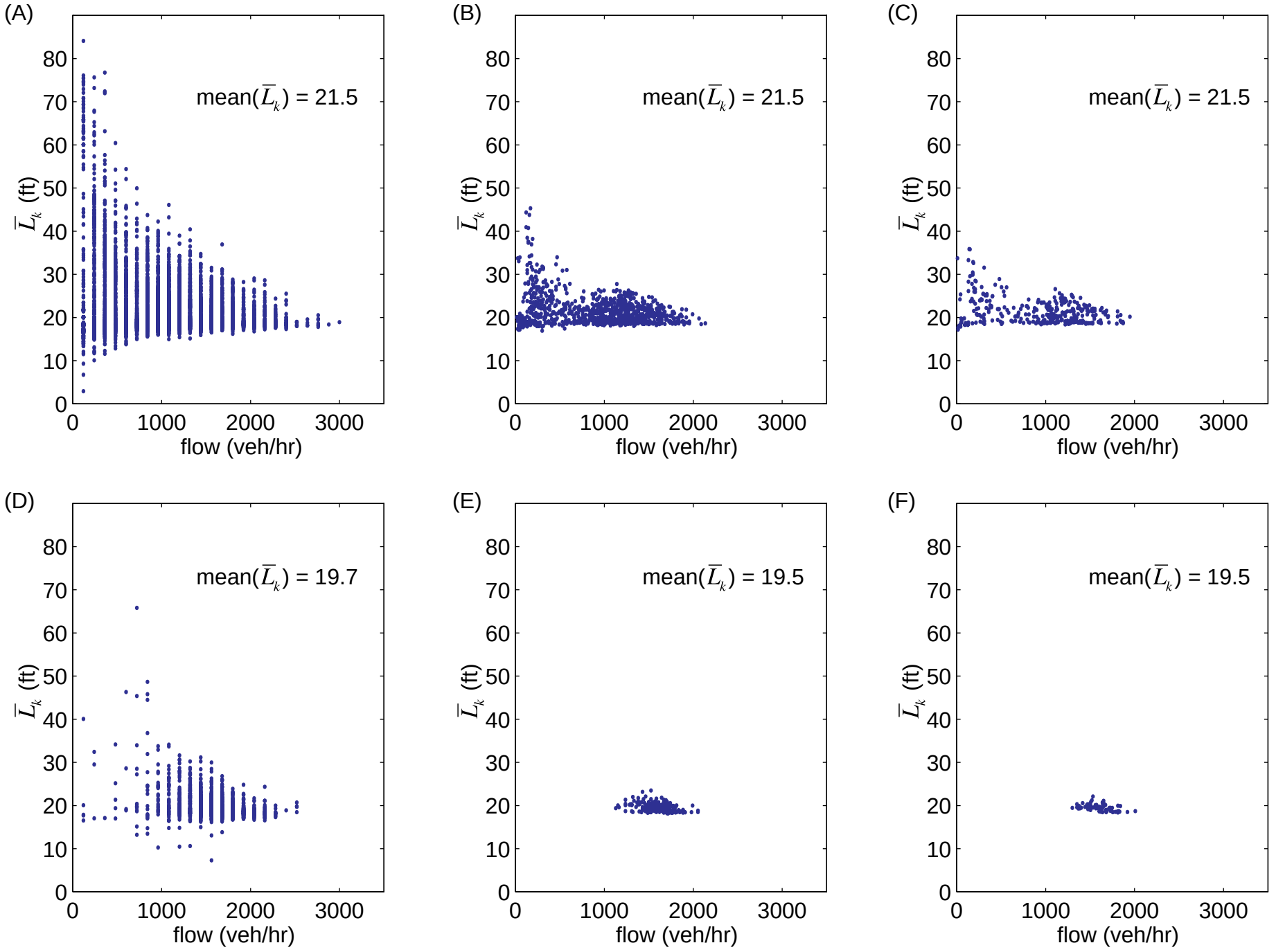

Figure 7, Estimated velocity versus measured velocity, northbound traffic, T = 30 sec, (A) lane 1, (B) lane 2, (C) lane 3, (D) lane 4.

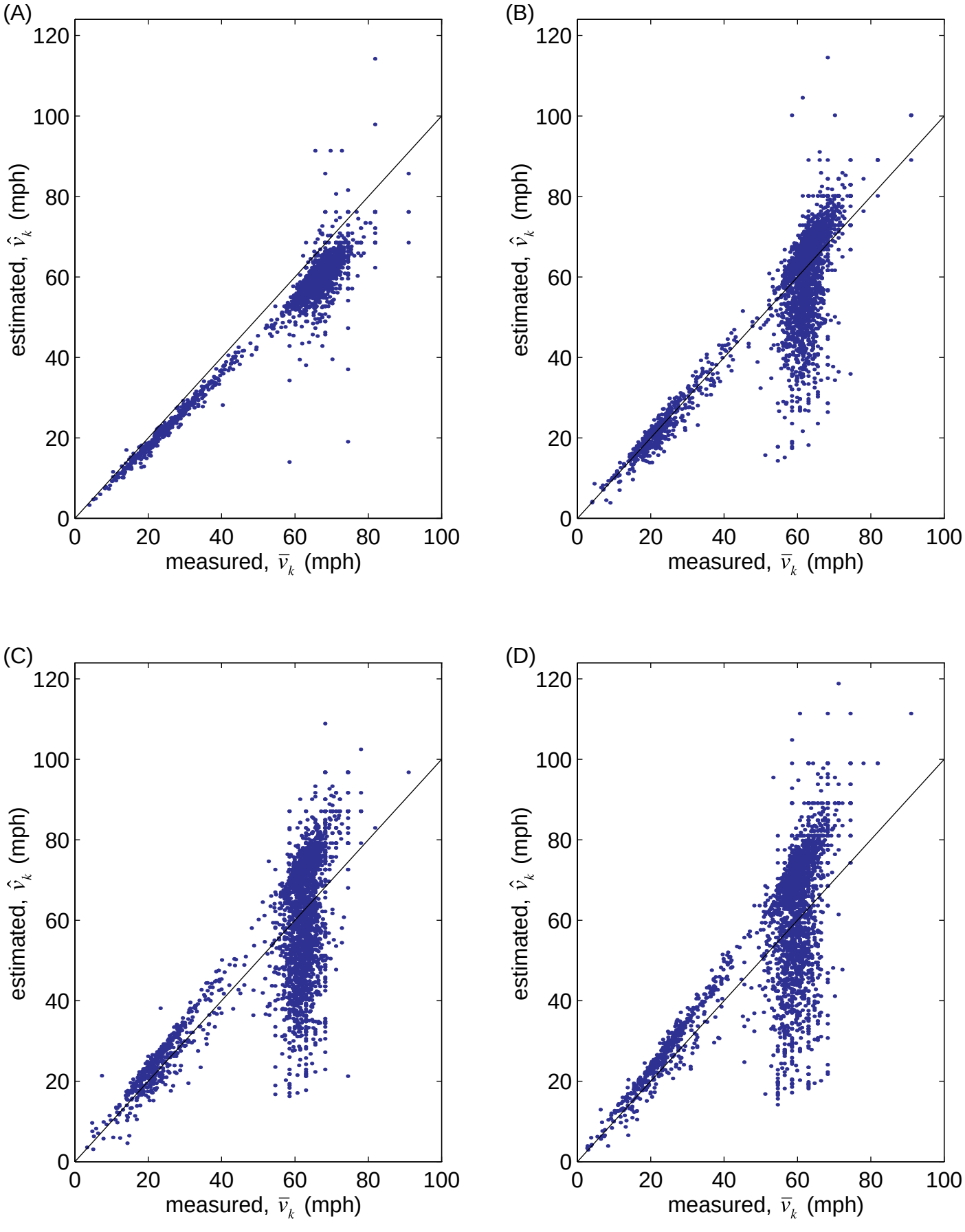

Figure 8, Estimated velocity versus measured velocity, northbound traffic, T = 5 min, (A) lane 1, (B) lane 2, (C) lane 3, (D) lane 4.

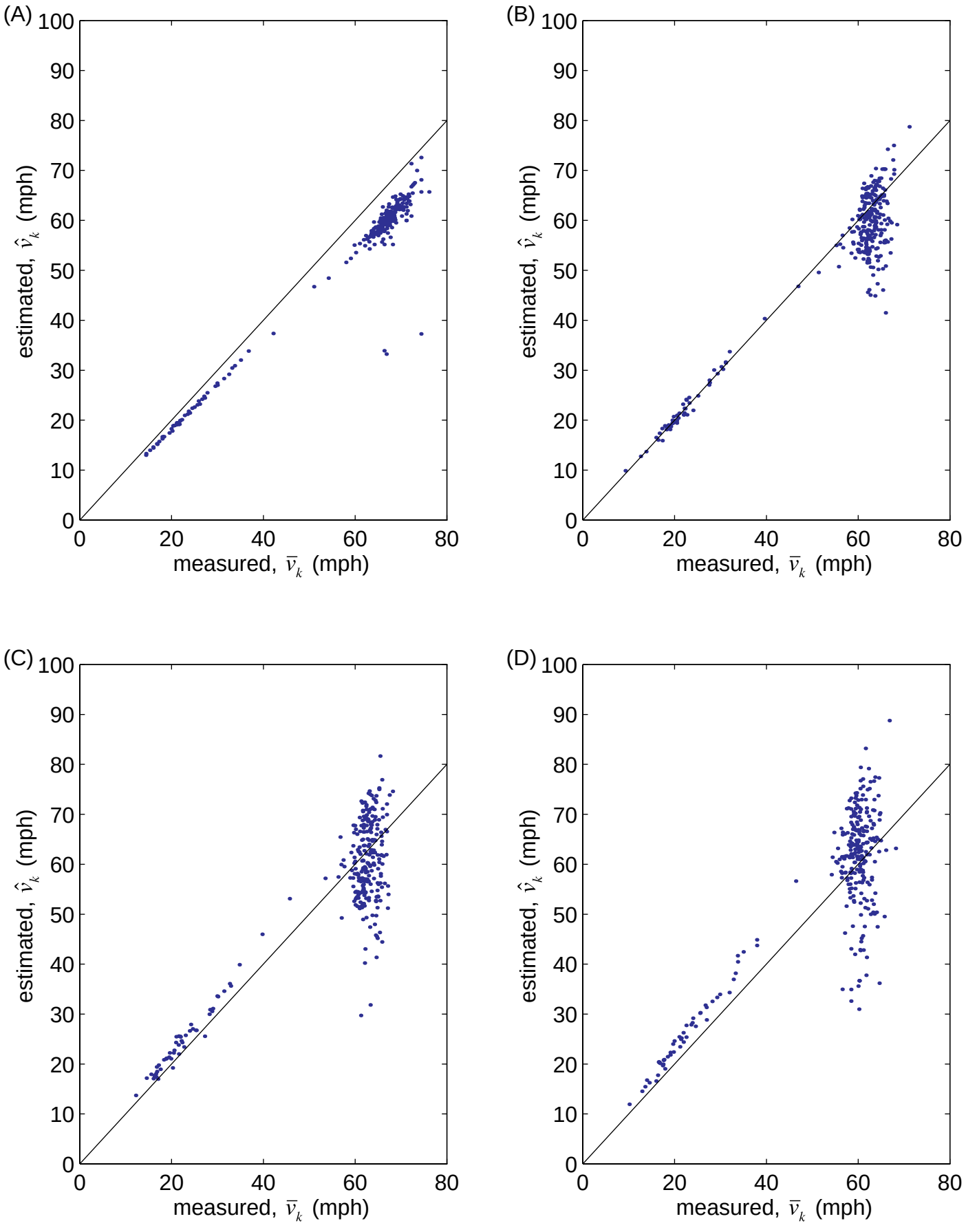

Figure 9, Contour plot showing the CDF of percent error in estimated velocity at fixed estimates of $\hat{L}$ for lane 1 northbound, +5% error for each line, (A) T = 30 sec, (B) T = 5 min.

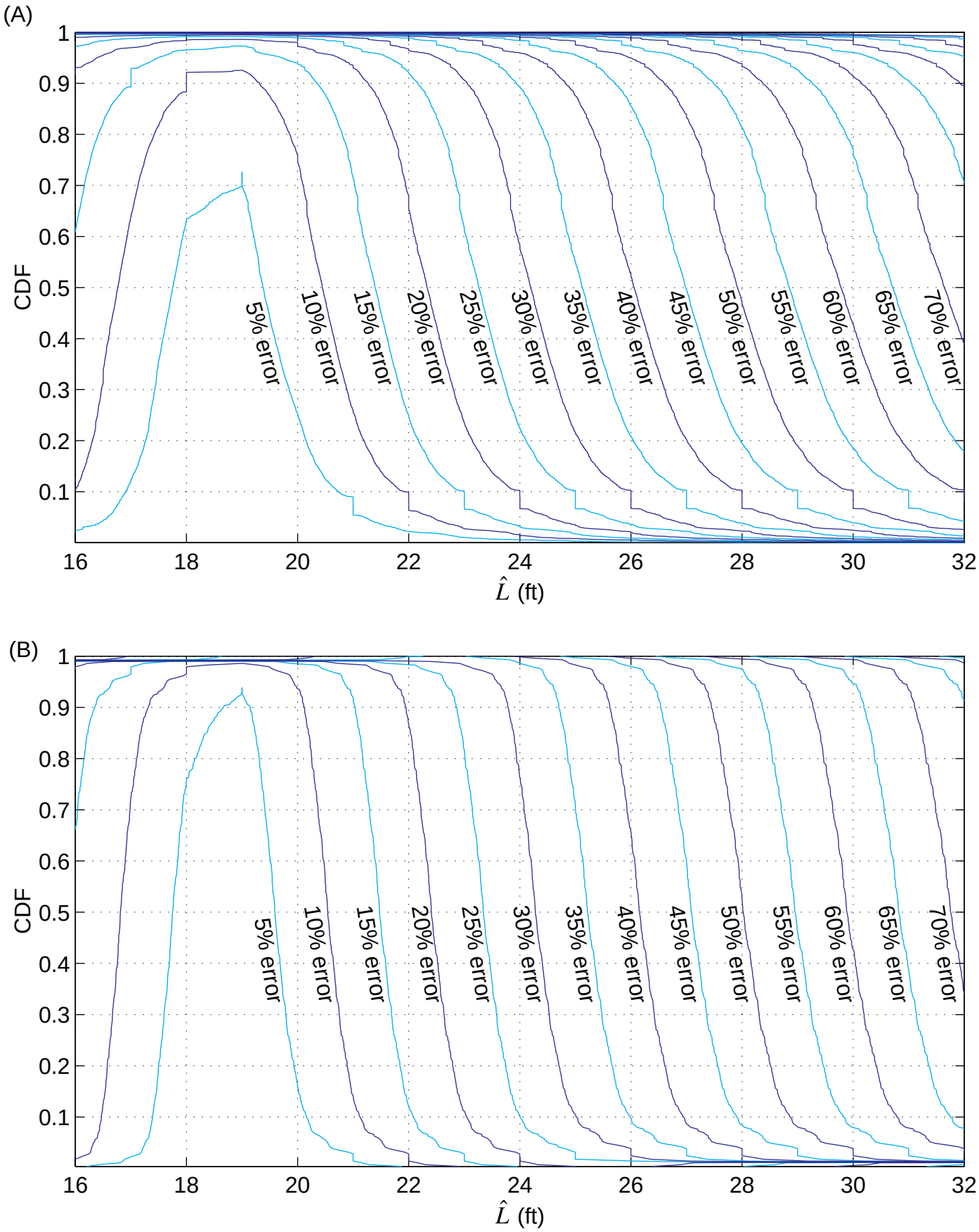

Figure 10, Contour plot showing the CDF of percent error in estimated velocity at fixed estimates of $\hat{L}$ for lane 5 southbound, +5% error for each line, (A) T = 30 sec, (B) T = 5 min.

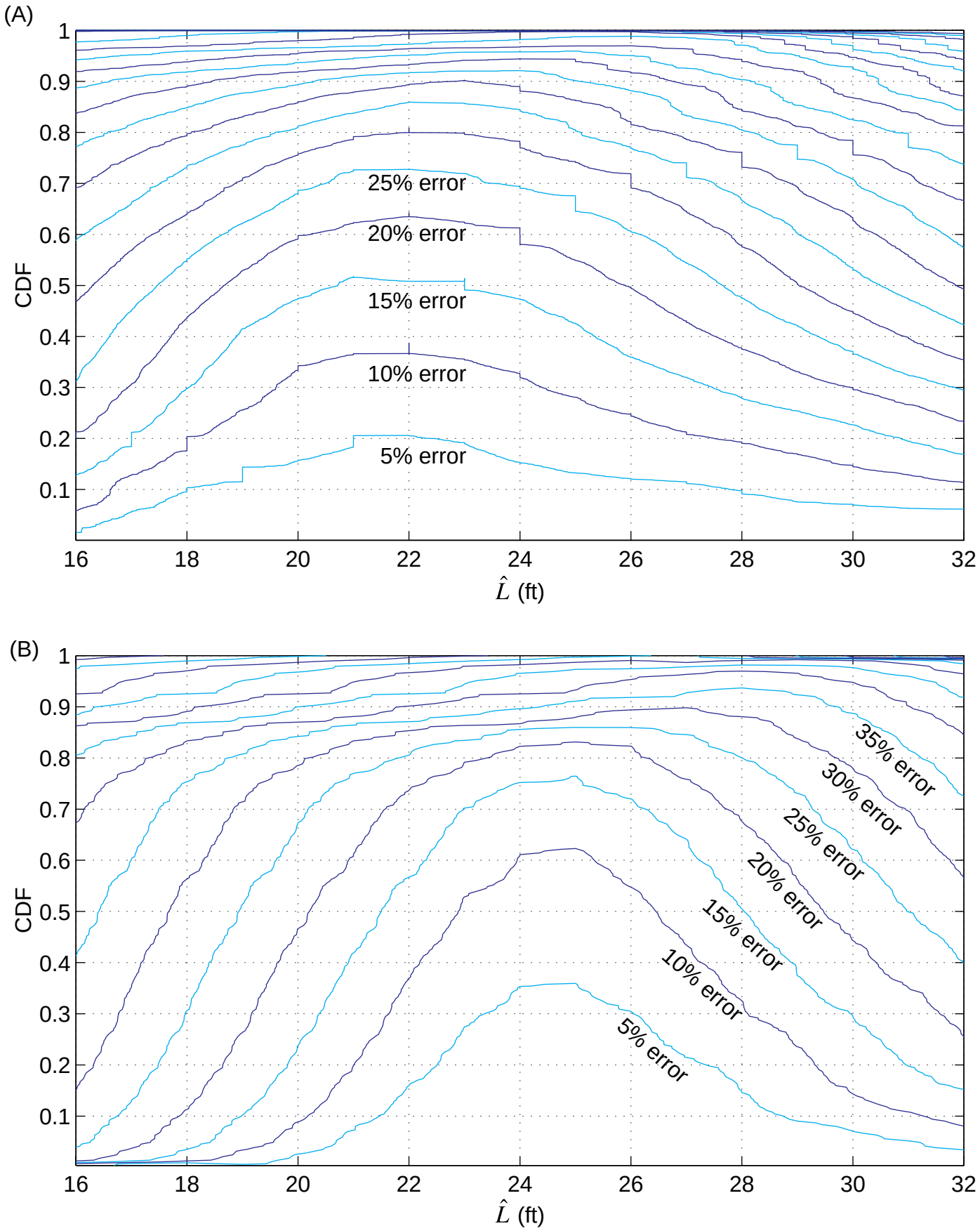

Figure 11, Simplified bivariate flow-occupancy relationship with observation k highlighted.

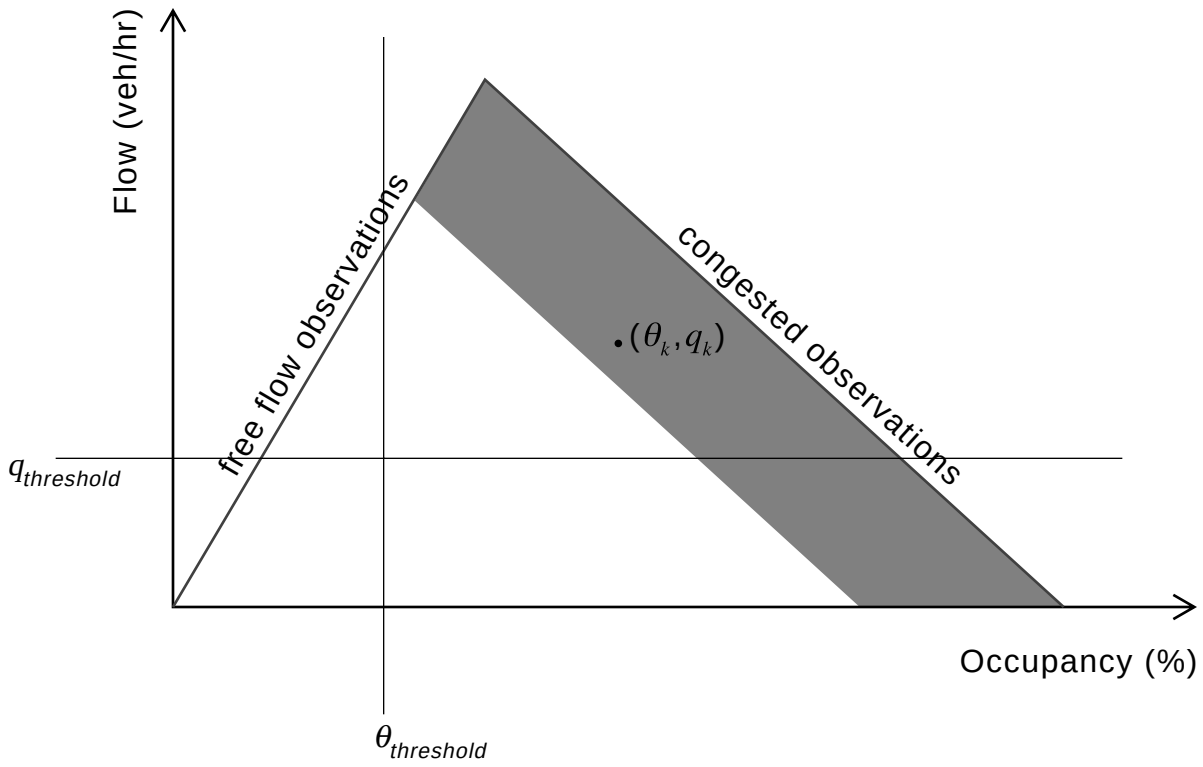

Figure 12,"Cleaned" estimated velocity versus measured velocity, northbound traffic, T = 5 min, (A) lane 1, (B) lane 2, (C) lane 3, (D) lane 4.

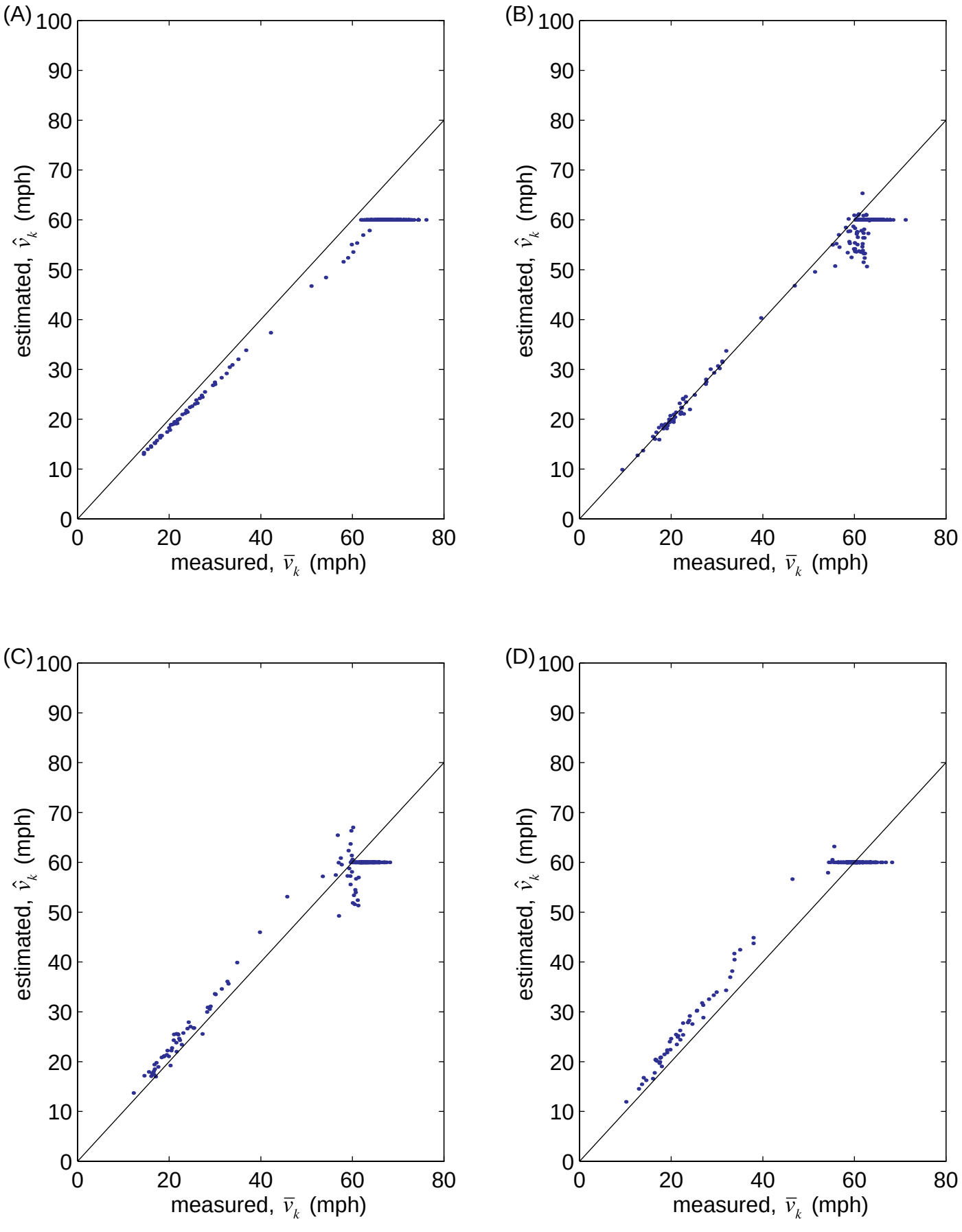

Figure 13, (A) Estimated velocity before cleaning, $\hat{v}_k$, northbound traffic, T = 5 min and the corresponding (B) estimates after cleaning, (C) measured velocities, $\bar{v}_k$.

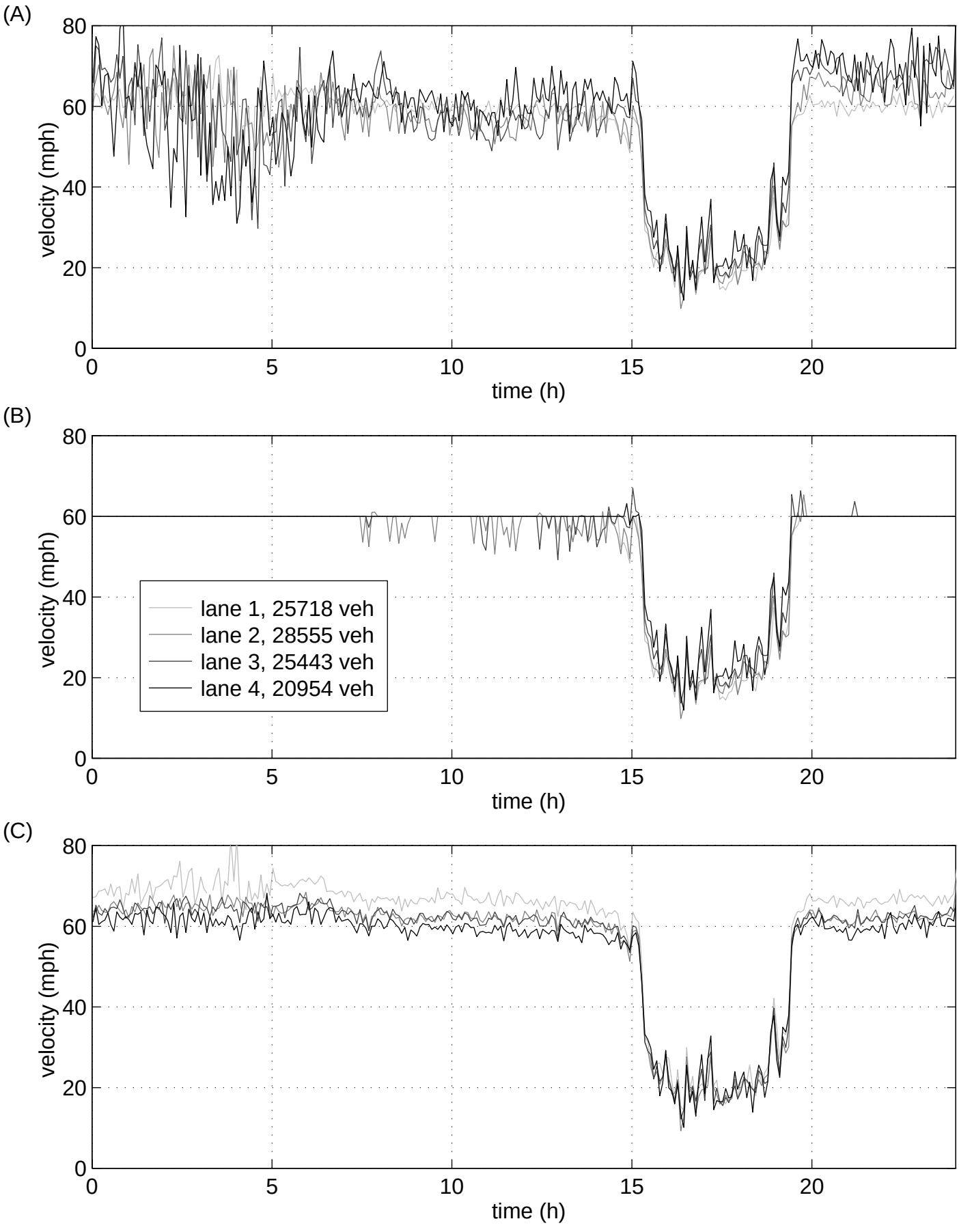

Figure 14, (A) Estimated velocity before cleaning, $\hat{v}_k$, southbound traffic, T = 5 min and the corresponding (B) estimates after cleaning, (C) measured velocities, $\bar{v}_k$.

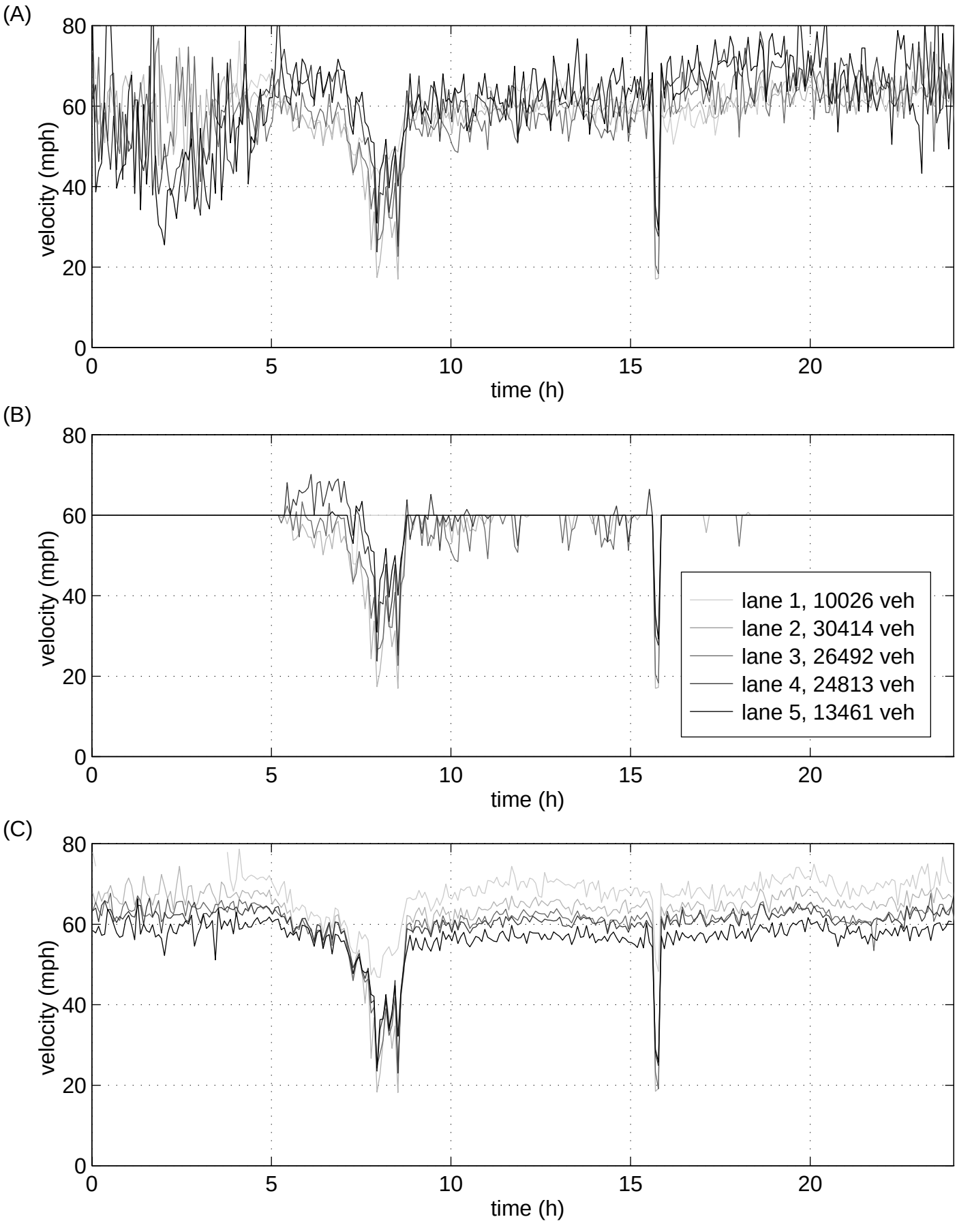

Figure 15, (A) Estimated velocity before cleaning, $\hat{v}_k$, southbound lane 3 (other lanes omitted for clarity), T = 30 sec and the corresponding (B) estimates after cleaning, (C) measured velocities, $\bar{v}_k$.

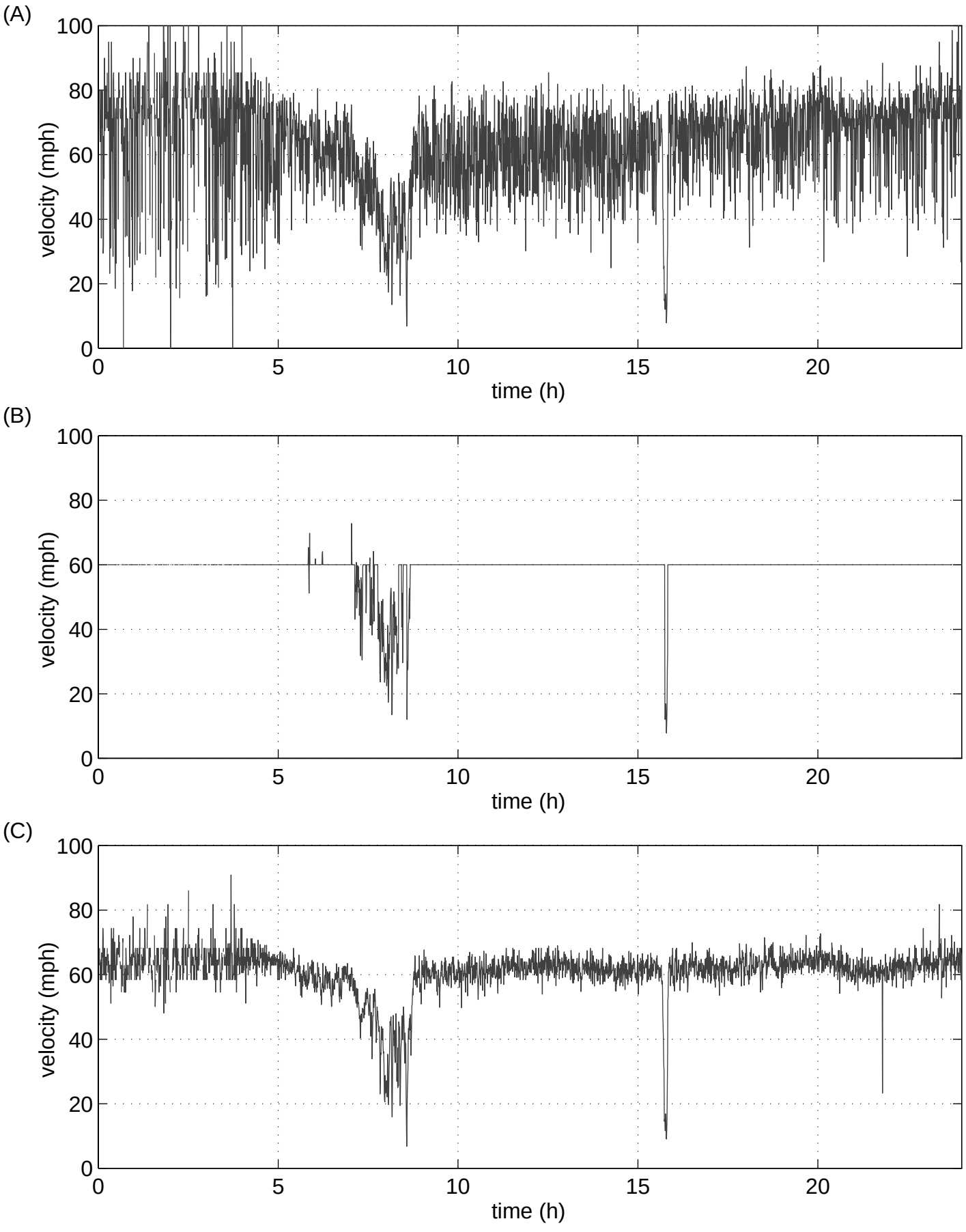

Figure 16, (A) The g-factor versus occupancy , T = 30 seconds, lane 1 northbound, (B) with occupancy rounded down to integer values, (C) using time mean speed and rounded occupancy.

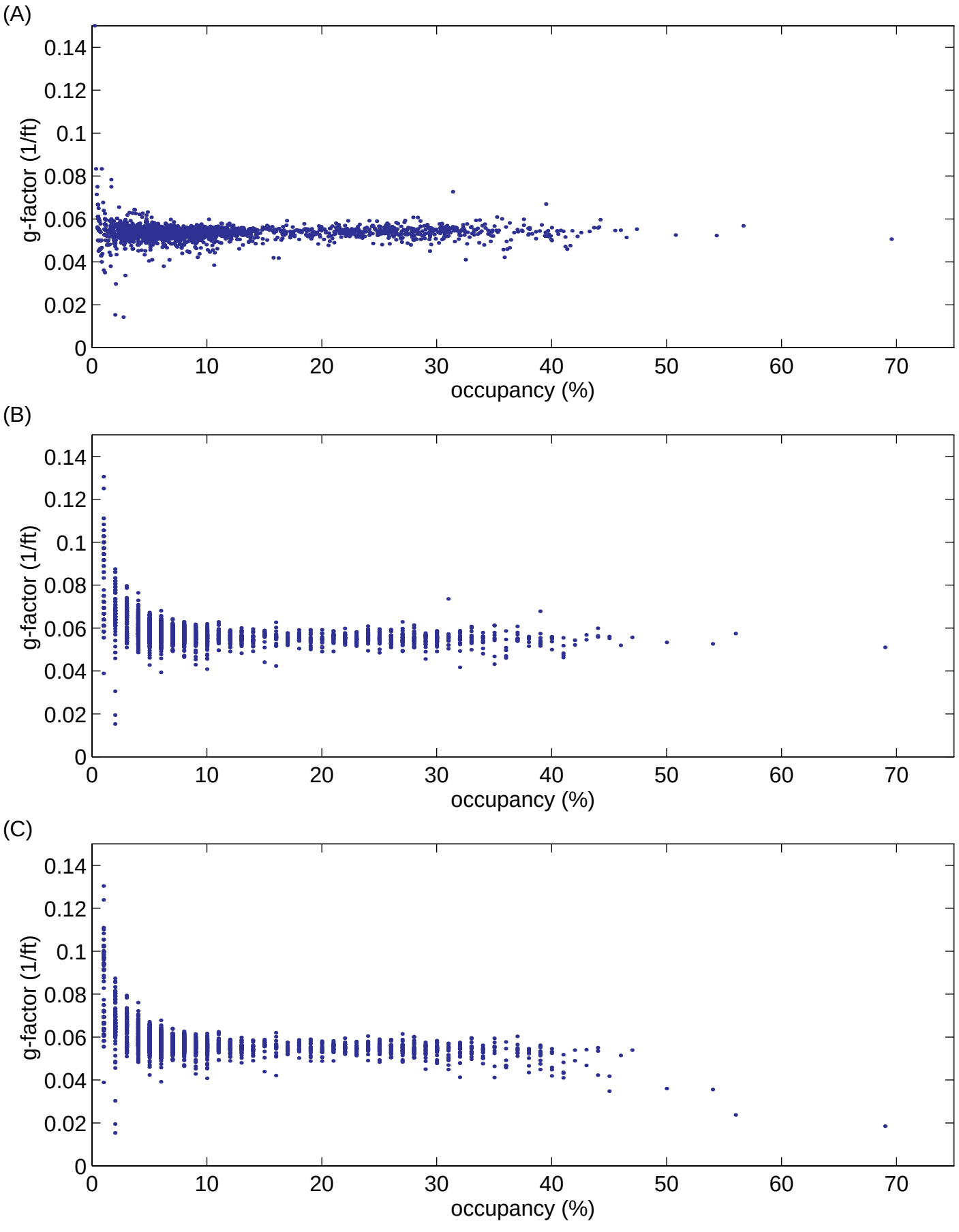

Figure 17, Mean g-factor calculated various ways versus occupancy , T = 30 seconds, northbound lane 1.

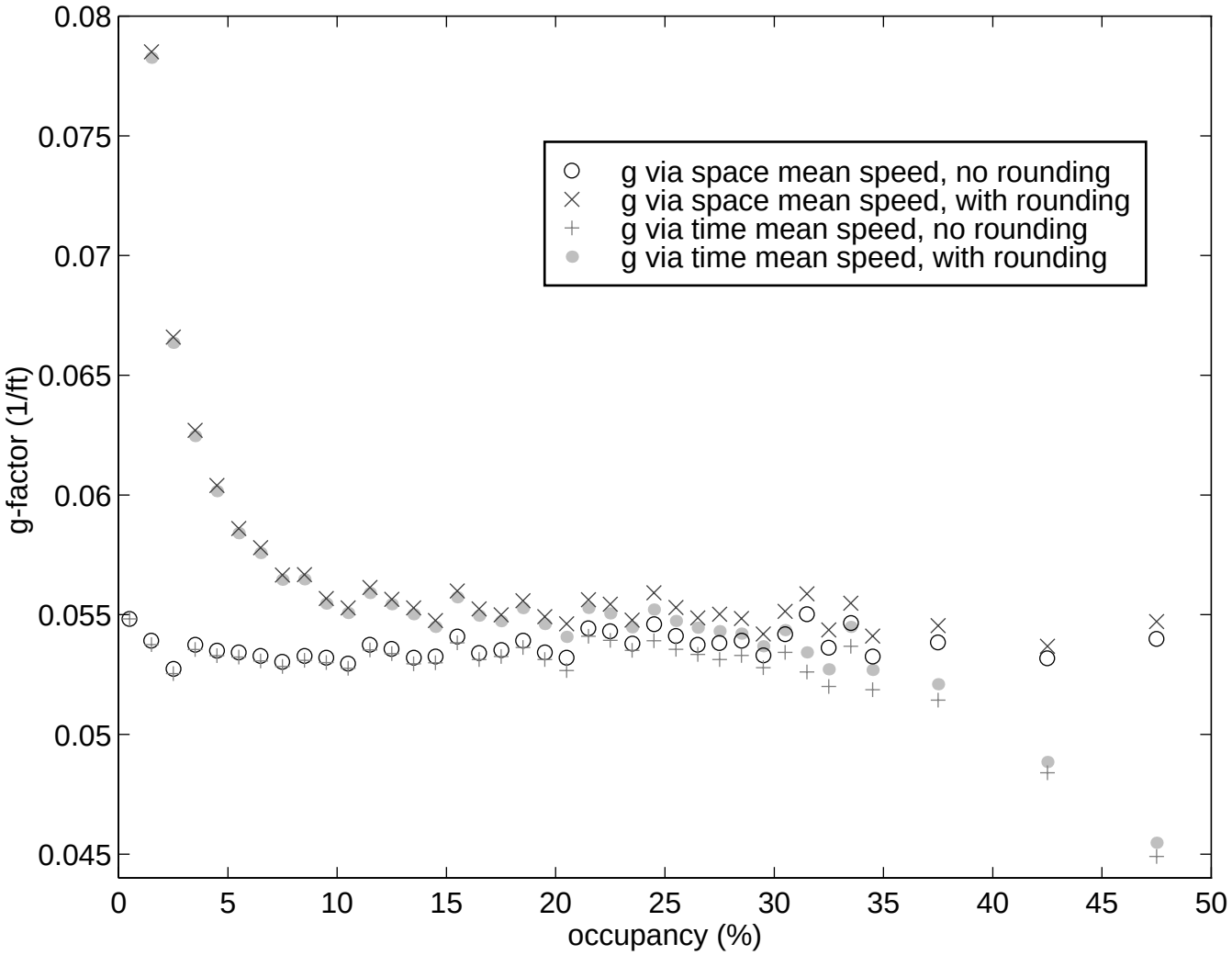

Table 1, The resulting estimates of $\hat{L}$ for the northbound traffic

Lane	$\hat{L}$ (feet) T = 30 sec	$\hat{L}$ (feet) T = 5 min
1	16.8	16.9
2	19.6	19.9
3	21.3	22.0
4	21.8	22.8